

Optical study of hot electron transport in GaN: Signatures of the hot-phonon effect

Kejia Wang, John Simon, Niti Goel, and Debdeep Jena^{a)}

Department of Electrical Engineering, University of Notre Dame, Notre Dame, Indiana 46556

(Received 21 September 2005; accepted 13 December 2005; published online 9 January 2006)

The hot-phonon lifetime in GaN is measured by temperature- and electric field-dependent photoluminescence studies of a *n*-type channel. The rate of increase of electron temperature with the external electric field provides a signature of non-equilibrium hot-phonon accumulation. Hot-electron temperatures are measured directly as a function of applied electric fields, and by comparing theoretical models for electron energy-loss into acoustic and optical phonons, a hot-phonon lifetime of $\tau_{ph}=3$ to 4 ps is extracted. © 2006 American Institute of Physics. [DOI: 10.1063/1.2163709]

The drift velocity of electrons in GaN has been observed in some recent reports¹ to be considerably lower than predicted by Monte Carlo simulations. Some other reports, however, claim the contrary.^{2,3} It has been proposed that the accumulation of nonequilibrium phonons (so-called “hot-phonons”) is responsible for the lowering of the drift velocity.⁴ A high drift velocity of carriers in the III-V nitrides is of paramount importance for a variety of applications in high-speed electronic and optical devices that operate via transport of hot electrons. In this work, we present direct measurement of electron temperatures in a doped GaN layer at low to moderate electric fields. We extract the hot-electron temperatures from the high-energy tails of the photoluminescence spectra for this purpose, and present strong evidence of the existence of hot-phonons by comparing the measured field-induced hot electron temperatures with theoretical models for energy loss mechanisms.

The rate of emission of LO phonons by electrons heated by an electric field is given by the polar Fröhlich interaction⁵

$$\frac{1}{\tau_{e-ph}} = \frac{e^2}{4\pi\hbar} \sqrt{\frac{2m^*\hbar\omega_{LO}}{\hbar^2}} \left(\frac{1}{\epsilon_\infty} - \frac{1}{\epsilon_0} \right), \quad (1)$$

where τ_{e-ph} is the electron-phonon interaction time, e is the electron charge, \hbar is the reduced Planck's constant, $\hbar\omega_{LO}=92$ meV is the LO-phonon energy in GaN, $m^*=0.2m_0$ is the electron effective mass in the Γ valley in GaN (m_0 is the free-electron mass), and ϵ_∞ and ϵ_0 are the high-frequency and dc dielectric constants in GaN, respectively. This evaluates to 9 fs for GaN (the same quantity is 108 fs in GaAs). On the other hand, the rate of decay of LO phonons by the anharmonic three-phonon (Ridley) process $LO \rightarrow TO+LA$ yields a LO-phonon lifetime in the range of $\tau_{ph}=1-5$ ps. This has been theoretically calculated by Ridley,⁶ and more recently by Srivastava *et al.*,⁷ and experimentally verified⁸ by Tsen *et al.* Therefore, τ_{ph} for GaN is of the same order as in GaAs. Thus, LO phonons are emitted ~ 12 times faster by each electron in GaN than in GaAs, yet they decay at roughly the same rate in both semiconductors. In addition, typical electron channels in AlGaIn/GaN two-dimensional electron gases (2DEGs) have much higher electron densities than in AlGaAs/GaAs 2DEGs, resulting in much more copious emission of polar optical phonons. Therefore, it is very reasonable to expect much stronger non-equilibrium or hot-

phonon accumulation effects in GaN as compared to GaAs.

For electron populations heated by electric fields, Matulionis *et al.* have extracted hot-electron temperatures from noise-measurements in AlGaIn/GaN polarization-induced 2DEGs.^{1,9} Shigekawa *et al.* applied a combination of electroluminescence (EL) and photoluminescence (PL) techniques to study the temperature variation across an AlGaIn/GaN heterostructure and concluded a large increase in temperature at high drain-source bias.¹⁰ However, they have not analyzed the data from the point of view of non-equilibrium phonon accumulation. Thus, there has been no optical study of the hot-phonon effect in biased III-V nitride structures—that is the subject of this letter.

A Si-doped *n*-type GaN sample grown by molecular beam epitaxy (MBE) was studied in this work. The sample was grown on a commercially available semi-insulating GaN-on sapphire template (from LumiLOG). The Si-doped channel is 100 nm thick with nominal Si doping of $N_D=10^{18}/\text{cm}^3$. Source-drain ohmic contacts were formed by deposition of Ti/Al/Ni/Au stack metal contacts followed by annealing, and different devices were separated by mesa-etching. The measurement setup for field-dependent PL is shown schematically in Fig. 1(a). The mobility and sheet carrier concentration were characterized by a temperature-dependent Hall measurement; the results are shown in Fig. 1(b). The distance between the source and drain was 1.2 mm.

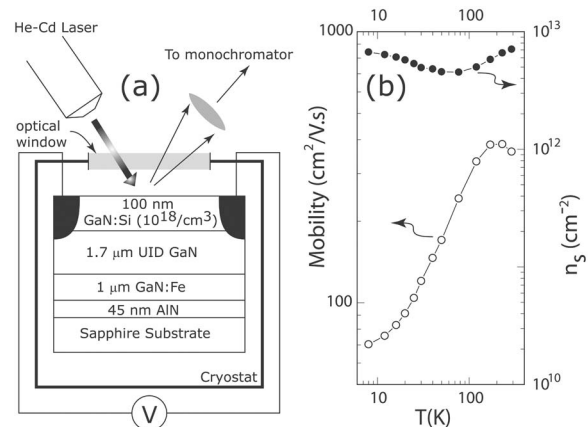


FIG. 1. (a) Setup for PL measurements, and (b) mobility and carrier concentration vs temperature of *n*-GaN MESFET structure from a Hall measurement. The mobility and carrier concentration are used for theoretical model of electron energy loss rates.

^{a)}Electronic mail: djena@nd.edu

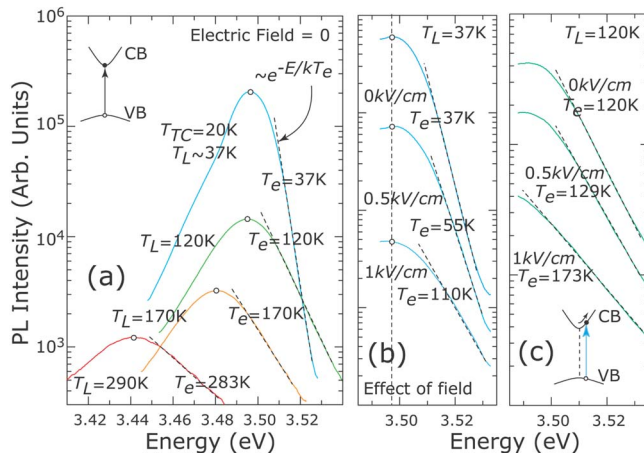


FIG. 2. (Color online) (a) PL spectra for four lattice temperatures at zero electric field, showing $T_e \approx T_L$, and PL spectra broadening with applied field at (b) $T_L = 37\text{ K}$ and (c) $T_L = 120\text{ K}$. The high energy tail fits an $\exp(-E/kT_e)$ variation accurately.

The sample was excited by a 325 nm He-Cd laser; the spot size was focused to about 0.4 mm diameter such that it excited the mesa only. The sample was kept in a closed-cycle He refrigerator with an optical window; the lattice temperature T_L was deduced from a thermocouple temperature T_{TC} . A dc voltage was applied across the ohmic contacts through leads connected by gold wire bonding, keeping the power $\leq 1\text{ W}$. The large area ensured efficient heat dissipation.

The PL spectra obtained are plotted in Fig. 2(a). The high energy tail of the PL spectra exhibits an exponential dependence on the excess photon energy ($\hbar\omega - E_G$) ($\hbar\omega$ is the photon energy and E_G is the bandgap) with a characteristic temperature which has been shown earlier to be the electron temperature T_e .¹¹ Note that as T_L increases, the interband transition PL peak red-shifts in accordance with the well-known Varshni empirical relation.¹² This gives a direct probe for both T_L and T_e , which is an advantage of the optical technique in such measurements.¹³

As shown earlier in the pioneering work by Shah *et al.*,¹¹ the high-energy tail of PL intensity spectra very closely follows the relation:

$$I_{\text{PL}} \propto D_j e^{-\frac{(\hbar\omega - E_g)}{k_B T_e}}, \quad (2)$$

where $D_j = \frac{1}{2\pi^2} (2\mu/\hbar^2)^{3/2} \sqrt{\hbar\omega - E_g}$ is the joint density of states,¹³ $1/\mu = 1/m_e^* + 1/m_h^*$ is the reduced effective mass, and k_B is the Boltzmann constant. Ideally, the intensity is proportional to the product of the hot-electron and hole-distributions $I \propto f_e f_h$; however, since the hole mass is large compared to electrons in GaN, it is neglected. We calibrate our measurements by observing that $T_L \approx T_e$ under zero applied field [Fig. 2(a)]. Except for the lowest temperature, this relation is indeed followed, and it justifies neglecting the contribution of holes. At the lowest temperature, the active channel is heated by the laser, and T_e at zero field is a more accurate measurement of T_L than T_{TC} .

With the application of an electric field across the channel, the spectra broadens as the electric field increases, and the electron temperature T_e is observed to increase as shown in Figs. 2(b) and 2(c). For nonzero electric fields, the PL measurements are taken sufficiently rapidly to ensure that the peak of the PL spectra does not shift as the dc field is applied, ensuring that T_L is constant over a measurement. The

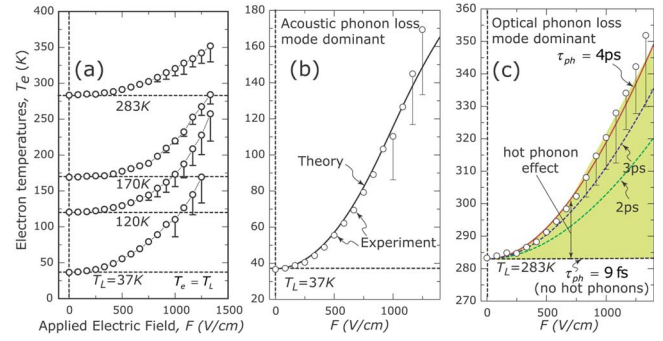


FIG. 3. (Color online) (a) Electron temperature T_e vs electric field at different lattice temperatures, and theoretical vs measured electron temperature for (b) $T_L = 37\text{ K}$ and (c) $T_L = 283\text{ K}$. The measured T_e values (empty circles) at $T_L = 283\text{ K}$ are best explained from the energy-loss model by a hot-phonon lifetime of $\tau_{\text{ph}} = 3$ to 4 ps.

shift of the PL peak due to increased electron temperature is of the order kT_e , which is negligible compared to the large bandgap of GaN. This is highlighted by the vertical dashed line in Fig. 2(b). The measurements were repeated for various lattice temperatures, with the electric field varying from 0 to 1400 V/cm. The electron temperatures T_e obtained are shown in Fig. 3(a); the error bars are estimated from fluctuations of T_e and T_L . The carrier temperature was observed to increase with applied electric field, with the rate of increase slowing down for higher lattice temperatures. This increase in T_e due to heating of electrons by the applied electric field may be explained by a simple model of energy conservation, which we briefly describe before analyzing the experimental data.

The energy that electrons gain from the applied electric field is lost to the crystal through inelastic collisions resulting in the creation of acoustic and optical phonons. It has been shown that the energy loss rate (ELR) to acoustic phonon modes (both deformation potential and piezoelectric) is given by¹⁴

$$P_{e,\text{ac}} = \frac{3(m^*)^2 k_F}{\pi \rho \hbar^3} \left(a_C^2 + \frac{2}{5} \frac{C_{\text{ac,tot}}^2}{k_F^2} \right) k_B (T_e - T_L), \quad (3)$$

where $k_F = (3\pi^2 n)^{1/3}$ is the Fermi wavevector (n being the three-dimensional carrier density), ρ is the mass-density of GaN, a_C is the conduction-band deformation potential, and $C_{\text{ac,tot}}$ is the directionally averaged piezoelectric coupling constant which includes both the longitudinal and transverse modes ($C_{\text{ac,tot}}^2 = C_{\text{LA}}^2 + C_{\text{TA}}^2$). The values for GaN used here can be found in the work of Stanton *et al.*,¹⁴ and are not quoted here.

Similarly, the ELR to LO-phonon modes assuming the experimentally verified first-order phonon decay process⁵ is given by¹⁵

$$P_{e,\text{LO}} = \frac{\hbar \omega_{\text{LO}}}{\tau_{\text{ph}}} \frac{e^{x_0 - x_e} - 1}{e^{x_0} - 1} \frac{\sqrt{x_e/2} e^{x_e/2} K_0(x_e/2)}{\sqrt{\pi/2}}, \quad (4)$$

where τ_{ph} is the effective LO-phonon lifetime, $x_0 = \hbar \omega_{\text{LO}}/k_B T_L$, $x_e = \hbar \omega_{\text{LO}}/k_B T_e$, and $K_0(\dots)$ is the modified Bessel function of order zero. $\tau_{\text{ph}} = \tau_{e-\text{ph}}$ in the absence of hot-phonons, and $\tau_{\text{ph}} > \tau_{e-\text{ph}}$ is a signature of the presence of nonequilibrium hot phonons.⁵ Figure 4 shows the calculated dependence of total ELR on the acoustic mode and optical

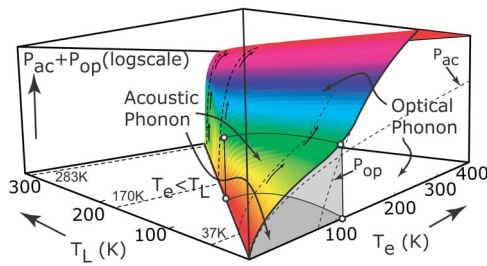


FIG. 4. (Color online) The total energy loss rate (ELR) is plotted along with the contributions of the acoustic and optical modes in the (T_e, T_L) parameter space. At very low lattice temperatures, the crossover from acoustic-phonon dominated ELR to LO-phonon dominated ELR occurs at $T_e \approx 110$ K. For $T_L \geq 100$ K, ELR is dominated by LO-phonon emission. The trajectories indicate some T_L values chosen in the PL measurements.

modes, and indicates that for $T_L \geq 100$ K, acoustic modes may be neglected.

The total energy gain rate from the electric field per electron $P_{e,\text{in}} = e\mu F^2$ (where μ is the mobility and F is the electric field) is set equal to the total ELR given by the sum $P_{e,\text{ac}} + P_{e,\text{LO}}$, and the equation is solved for the dependence of T_e on F for a fixed T_L .¹⁶ For each T_L , the experimental carrier density and the mobility shown in Fig. 1(b) is used. The calculated and measured electron temperatures for lattice temperatures of $T_L = 37$ K and $T_L = 283$ K are shown in Figs. 3(b) and 3(c), respectively.

It is found that the simple model outlined above is able to explain the measured electron temperature variation with electric field rather well. For $T_L = 37$ K, ELR through optical modes is negligible for $T_e \leq 110$ K, the process being dominated by the combined deformation-potential and piezoelectric acoustic modes, as confirmed from the agreement of measured and calculated values in Fig. 3(b). For $T_e > 110$ K, the rate of increase of T_e with field slows down due to the onset of LO phonon emission as indicated in the calculated T_e in Fig. 3(b) (also see Fig. 4). However, due to lattice heating by the electric field, we encounter significant fluctuations in the measured T_e values as indicated by the error bars, and hence do not claim to observe this transition.

We now turn to measuring hot-phonon lifetime, which is the main subject of this work. It is done by calculating the T_e

variation with F for different τ_{ph} values, and finding the value that best explains the measured data. In Fig. 3(c), we show the measured T_e versus F along with the calculated T_e for $T_L = 283$ K. Four calculated lines are plotted—for $\tau_{\text{ph}} = \tau_{e-\text{ph}} = 9$ fs (no hot-phonon effect), and 2, 3, and 4 ps. From the fit, we conclude that $\tau_{\text{ph}} = 3$ to 4 ps within limits of experimental error. The value measured is close to those reported by Tsen *et al.*,⁸ and is in accordance with reports by noise-temperature measurements by Matulionis *et al.* as well.⁹ Thus, our measurement confirms the presence of nonequilibrium hot phonons in the low-field regime at temperatures close to the ambient.

The authors gratefully acknowledge financial support from the Office of Naval Research (Dr. C. Wood), and the University of Notre Dame research funds. The authors acknowledge useful discussions with Dr. A. Matulionis on the topic of hot-phonons.

- ¹M. Ramonas, A. Matulionis, J. Liberis, L. F. Eastman, X. Chen, and Y.-J. Sun, *Phys. Rev. B* **71**, 075324 (2005).
- ²J. M. Barker, D. K. Ferry, D. D. Koleske, and R. J. Shul, *J. Appl. Phys.* **97**, 063705 (2005).
- ³J. M. Barker, D. K. Ferry, S. M. Goodnick, D. D. Koleske, and R. J. Shul, *J. Vac. Sci. Technol. B* **22** (4), 2045 (2004).
- ⁴B. K. Ridley, W. J. Schaff, and L. F. Eastman, *J. Appl. Phys.* **96**, 1499 (2004).
- ⁵B. K. Ridley, *Semicond. Sci. Technol.* **4**, 1142 (1989).
- ⁶B. K. Ridley, *J. Phys.: Condens. Matter* **8**, L511 (1996).
- ⁷S. Barman and G. P. Srivastava, *Phys. Rev. B* **69**, 235208 (2004).
- ⁸K. T. Tsen, D. K. Ferry, A. Botchkarev, B. Sverdlov, A. Salvador, and H. Morkoc, *Appl. Phys. Lett.* **72**, 2132 (1998).
- ⁹A. Matulionis, *Hot Carriers in Semiconductors Conference*, Chicago (in press).
- ¹⁰N. Shigekawa, K. Shiojima, and T. Suemitsu, *J. Appl. Phys.* **92**, 531 (2002).
- ¹¹J. Shah, A. Pinczuk, A. C. Gossard, and W. Wiegmann, *Phys. Rev. Lett.* **54**, 2045 (1985).
- ¹²Y. P. Varshni, *Physica (Amsterdam)* **34**, 149 (1967).
- ¹³P. Yu and M. Cardona, *Fundamentals of Semiconductors: Physics and Material Properties*, 2nd ed. (Springer-Verlag, Berlin, 1998).
- ¹⁴N. M. Stanton, A. J. Kent, A. V. Akimov, P. Hawker, T. S. Cheng, and C. T. Foxon, *J. Appl. Phys.* **89**, 973 (2001).
- ¹⁵H. Ye, G. W. Wicks, and P. M. Fauchet, *Appl. Phys. Lett.* **74**, 711 (1999).
- ¹⁶G. Bauer and H. Kahlert, *Phys. Rev. B* **5**, 566 (1972).